Supporting information

Bimetallic Nanoparticles confined in an N-Doped Graphitic Carbon Shell: A High-Performance Trifunctional Catalyst for Efficient Water Splitting

Rajeshree J. Bani[a,b], Jyotiranjan Mishra[b,c], Sanjay Pratihar[b,c], Rajesh Patidar[b,d], Divesh N. Srivastava[a,b], and Gopala Ram Bhadu[a,b]

[a]*Marine Elements and Marine Environment Division, CSIR-Central Salt & Marine Chemicals Research Institute, G. B. Marg, Bhavnagar, 364002, Gujarat, India*

[b]*Academy of Scientific and Innovative Research (AcSIR), Ghaziabad, 201002, India*

[c]*Inorganic Materials and Catalysis Division, CSIR-Central Salt & Marine Chemicals Research Institute, G. B. Marg, Bhavnagar, 364002, Gujarat, India*

[d]*CSIR-Advanced Materials and Processes Research Institute, Bhopal, 462026, Madhya Pradesh, India*

Table of Contents

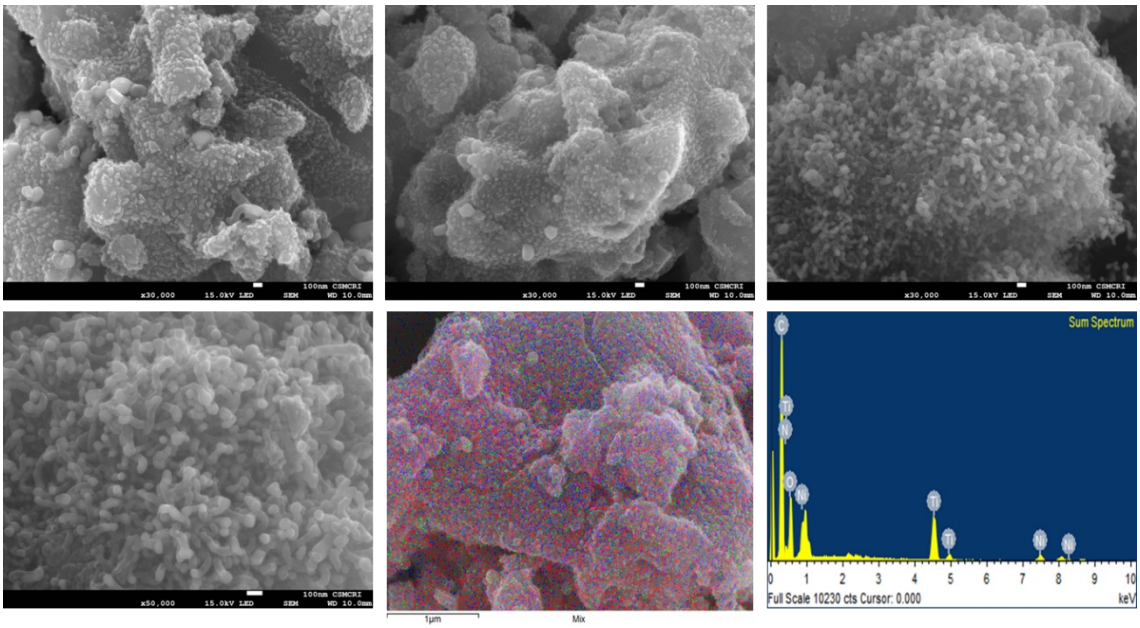

Figure S1. FE-SEM images, elemental mapping and EDX of NT@NC-7.

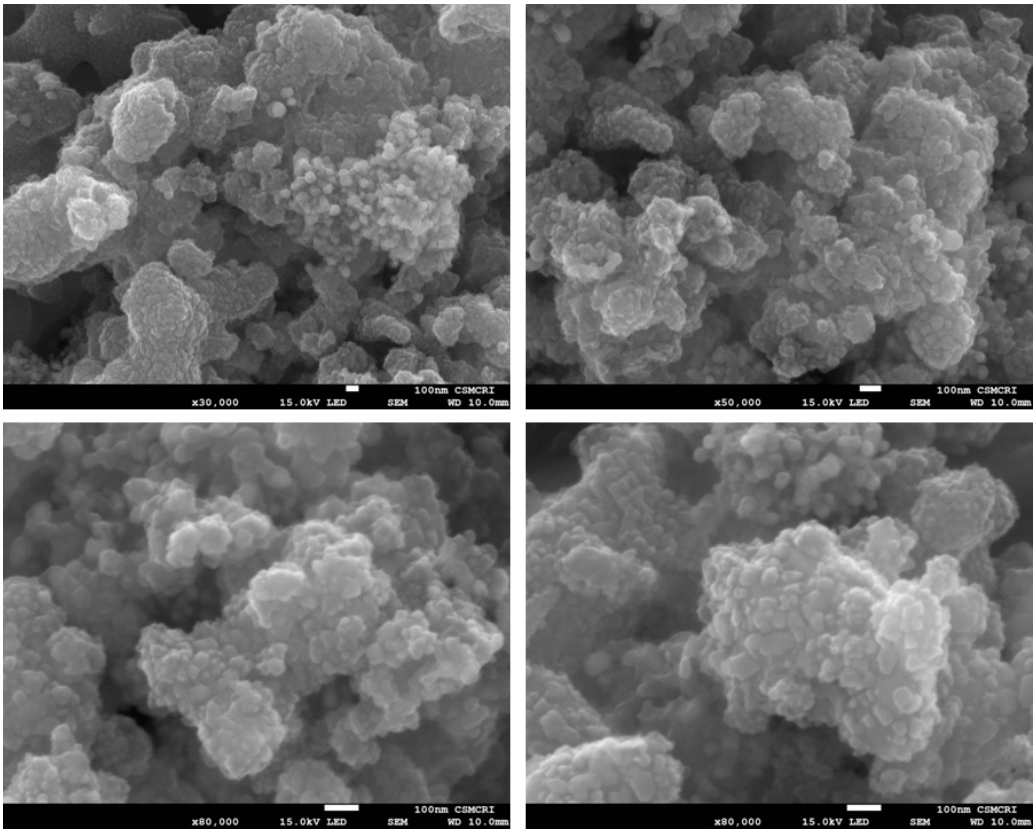

Figure S2. FE-SEM images of NT@NC-8.

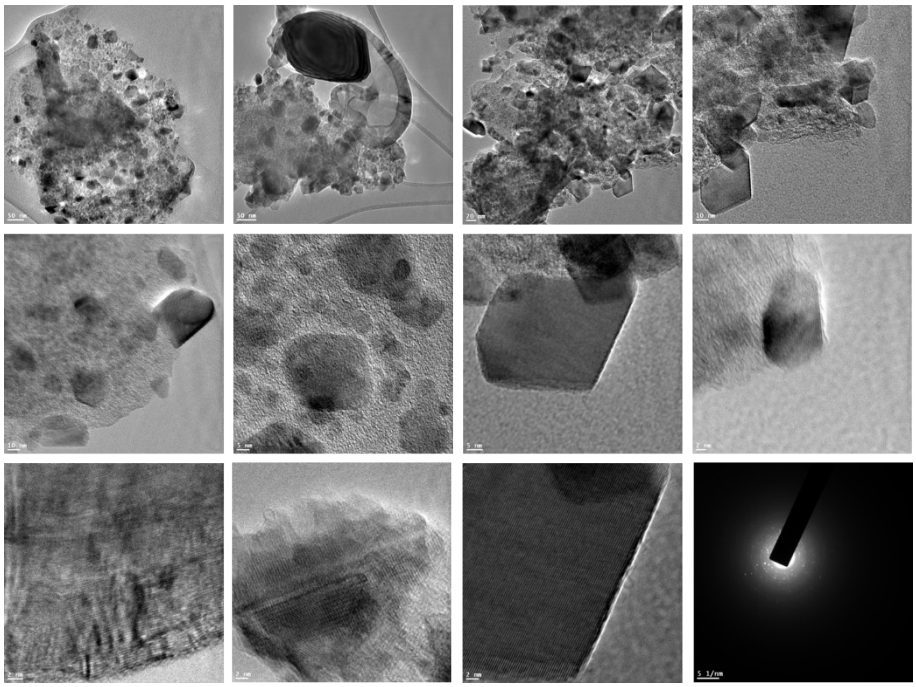

Figure S3. HR-TEM images of NT@NC-7.

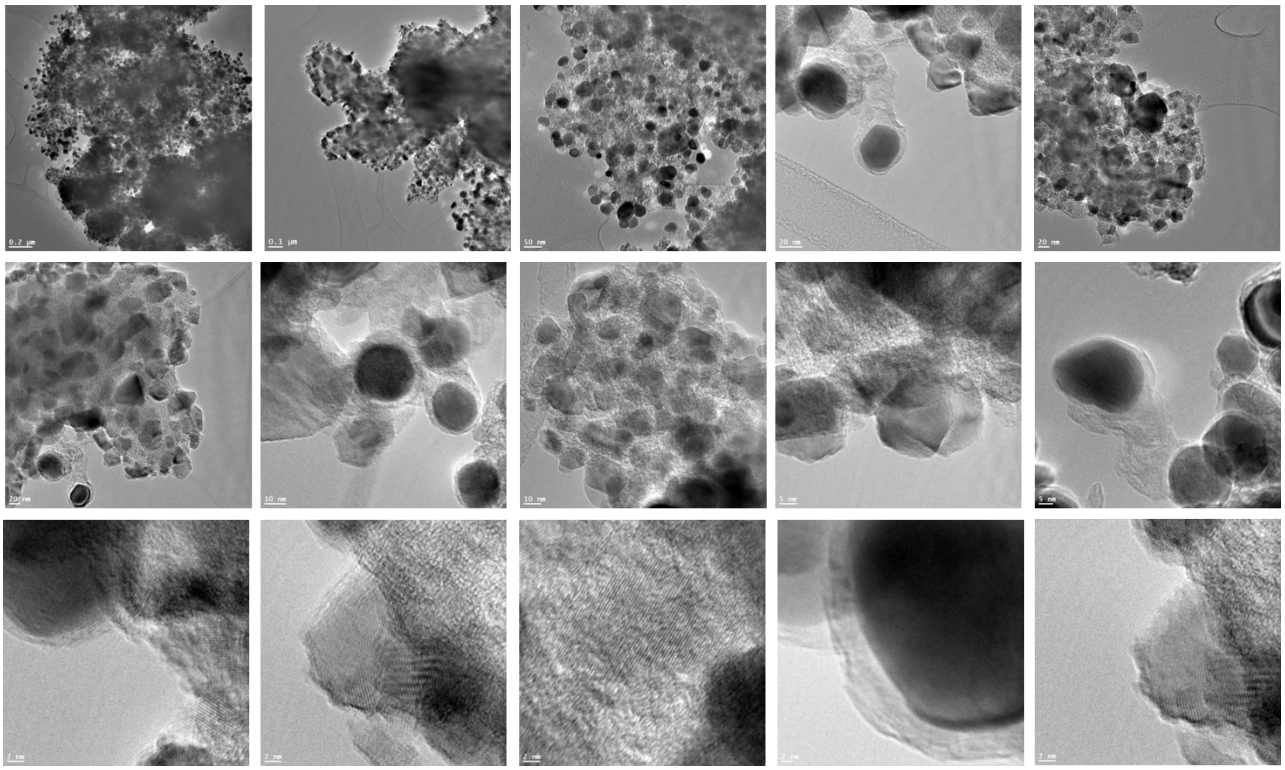

Figure S4. HR-TEM images of NT@NC-8.

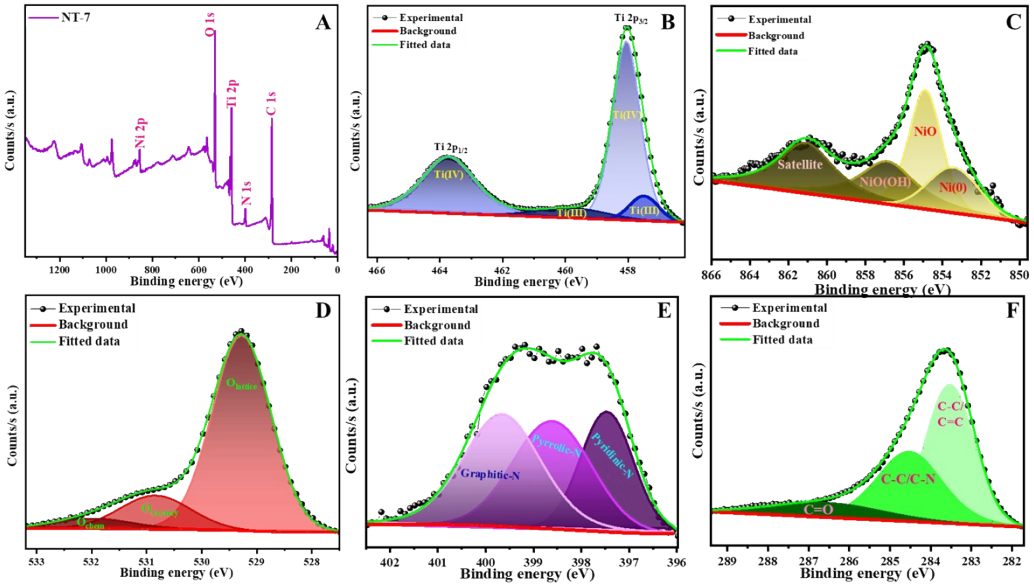

Figure S5. (A) XPS survey spectrum of NT@NC-7; Deconvoluted high resolution spectrum of (B) Ti 2p, (C) Ni 2p, (D) O 1s, (E) N 1s, and (F) C 1s of NT@NC-7.

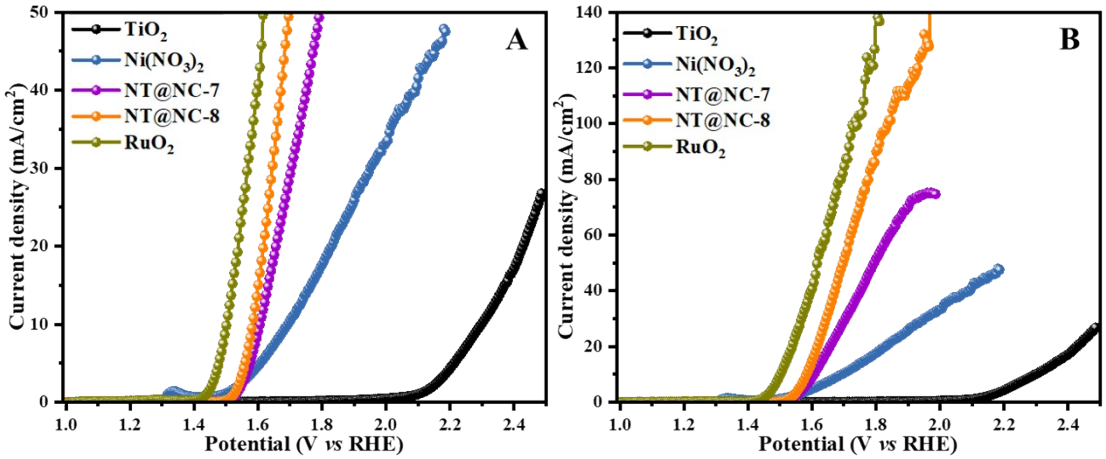

Figure S6. Linear sweep voltammograms for TiO_2, $Ni(NO_3)_2$, NT@NC-7, NT@NC-8 and RuO_2 showing OER current density upto (A) 50 mA/cm^2 (B) 140 mA/cm^2

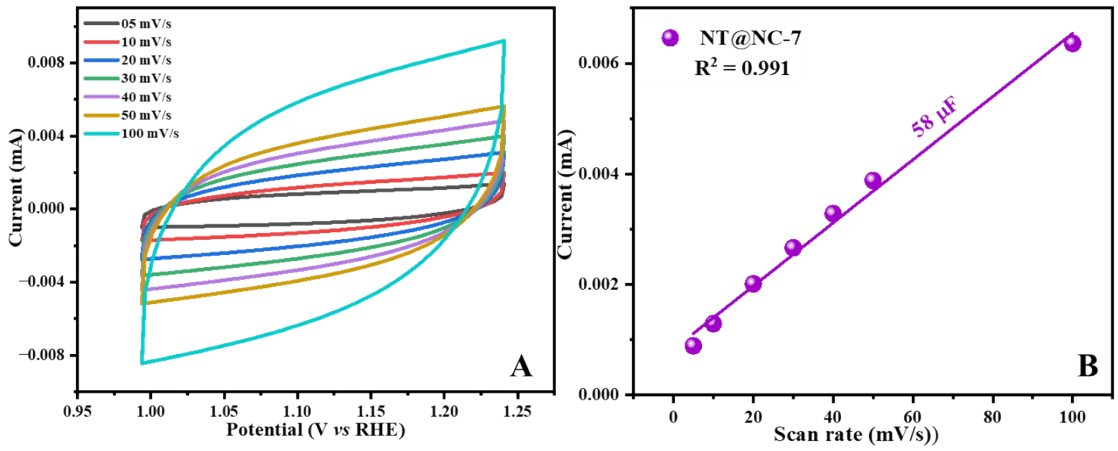

Figure S7. (A) Cyclic voltammograms of NT@NC-7 at different scan rates (B) the corresponding current (mA) vs scan rate (mV/s) plot to determine C_{dl}.

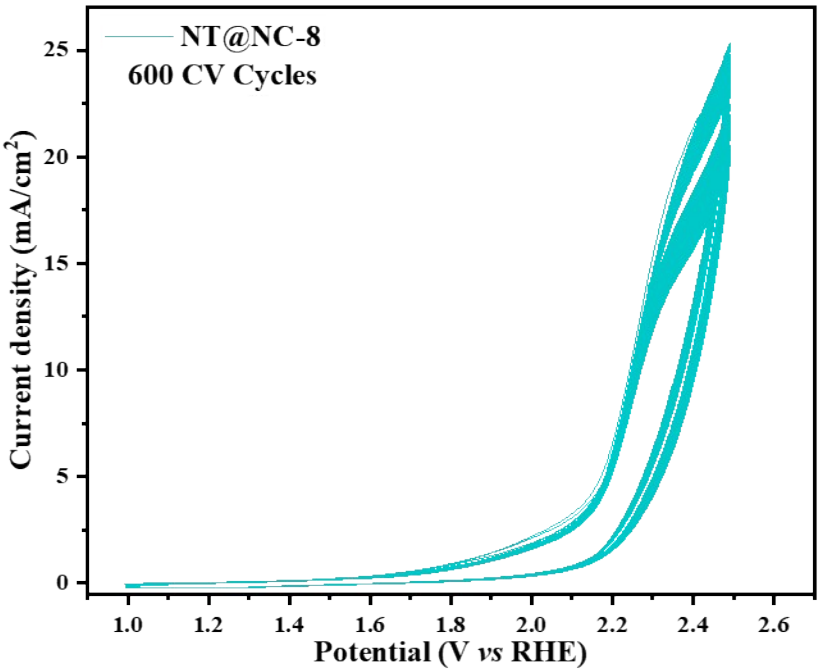

Figure S8. Cyclic voltammogram representing 600 CV cycles to test stability of NT@NC-8 catalyst.

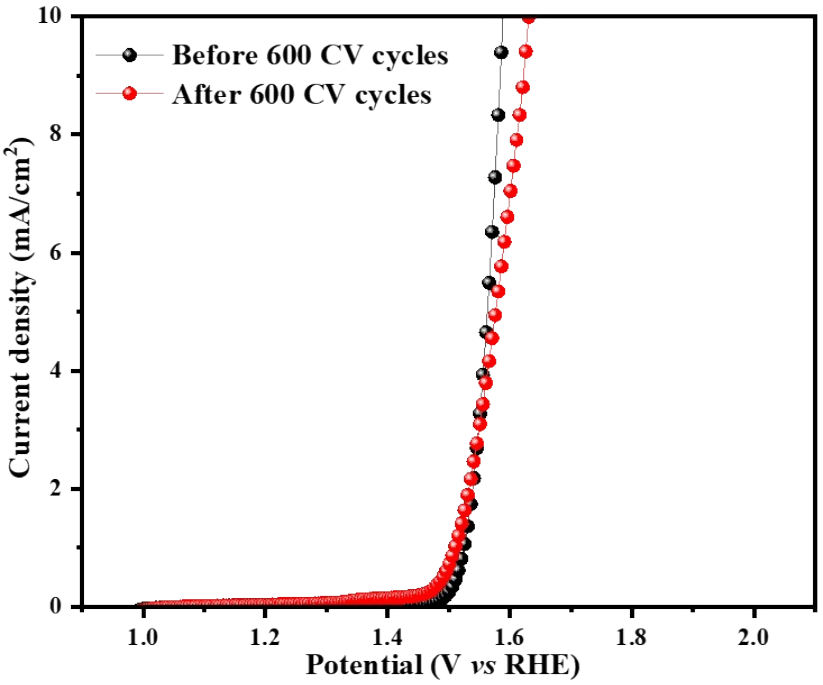

Figure S9. LSV curves before and after 600 CV cycles to analyze stability of NT@NC-8 catalyst.

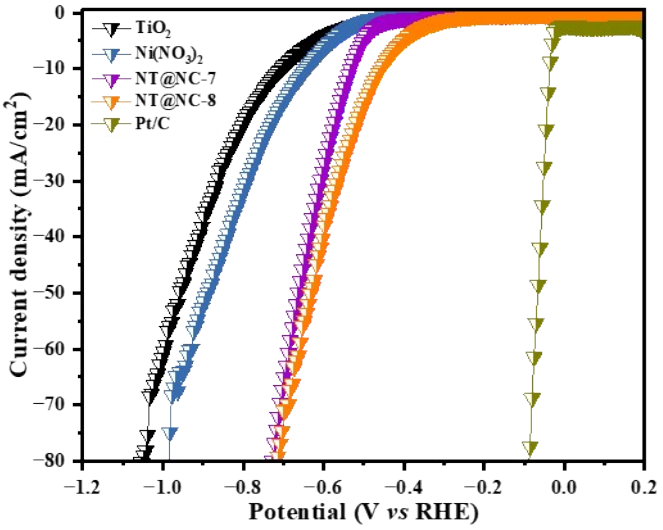

Figure S10. Linear sweep voltammograms for TiO_2, $Ni(NO_3)_2$, NT@NC-7, NT@NC-8 and Pt/C in 0.5 M H_2SO_4 showing HER current density upto 80 mA/cm^2.

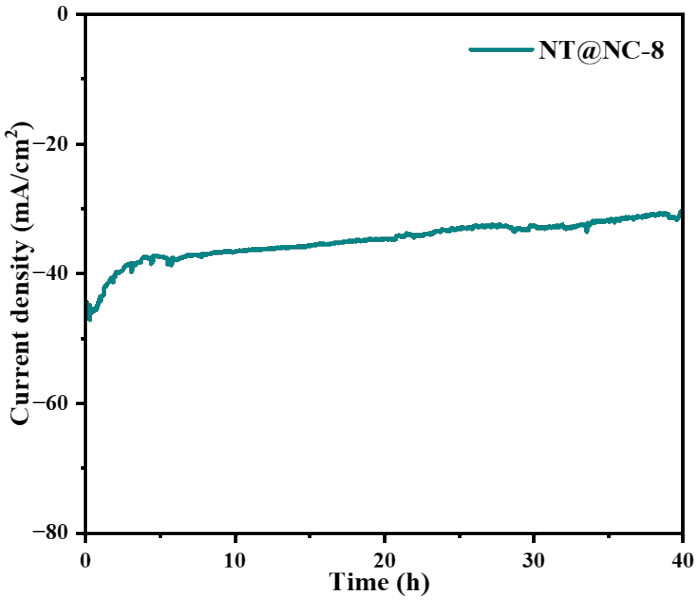

Figure S11. Chronoamperometric measurements to test HER stability in 0.5 M H_2SO_4 for 40 hr at -800 mV (vs Ag/AgCl).

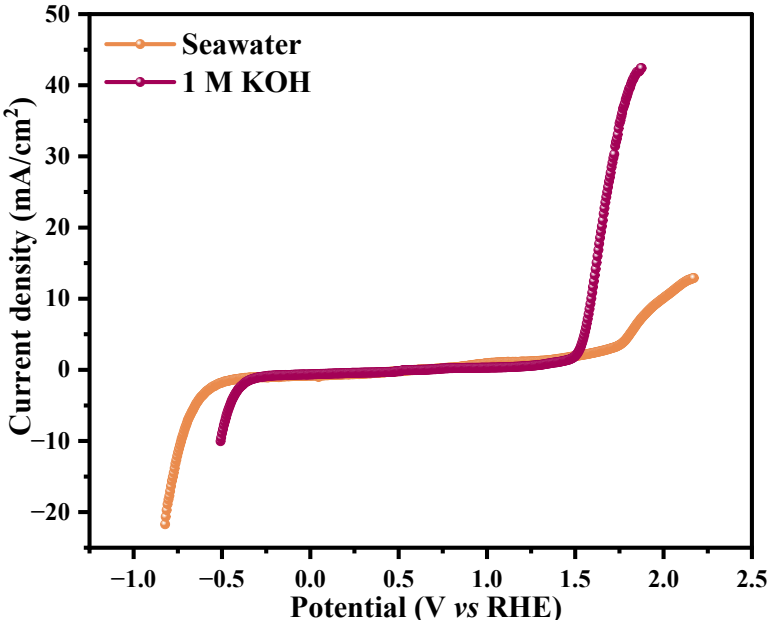

Figure S12. Overall water splitting using NT@NC-8 catalyst in 1 M KOH as well as in natural untreated seawater.

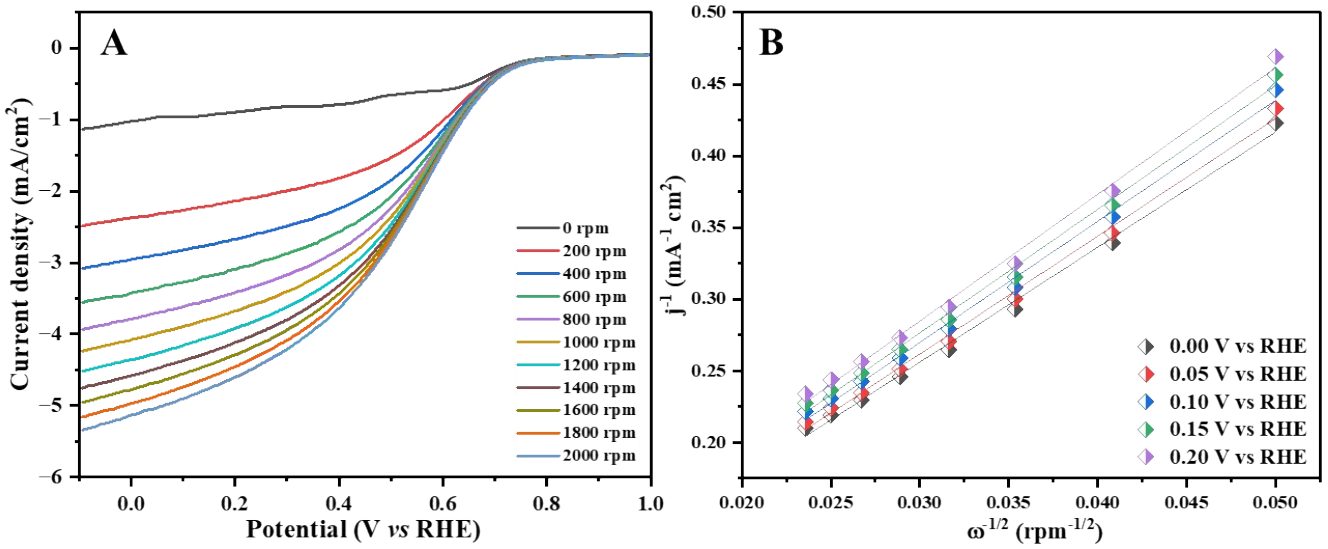

Figure S13. ORR analysis of NT@NC-7. (A) ORR LSV curves of NT@NC-7 at different rotation rates (0 to 2000 rpm). (B) the corresponding Koutecky–Levich plot of NT@NC-7.

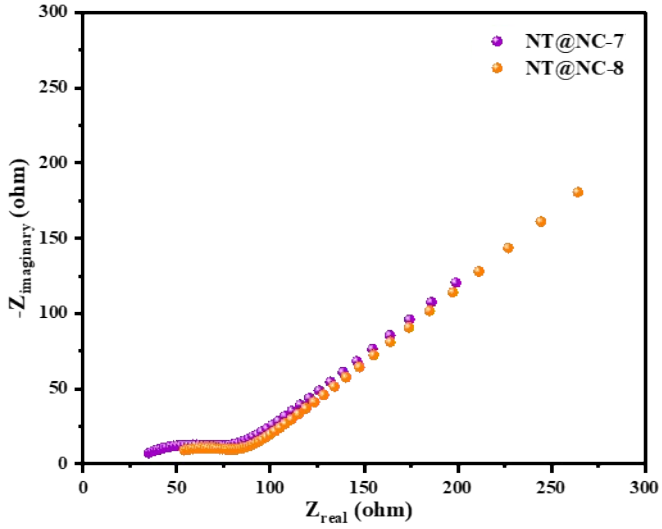

Figure S14. EIS plot of NT@NC-7 and NT@NC-8 in 0.1 M KOH electrolyte.

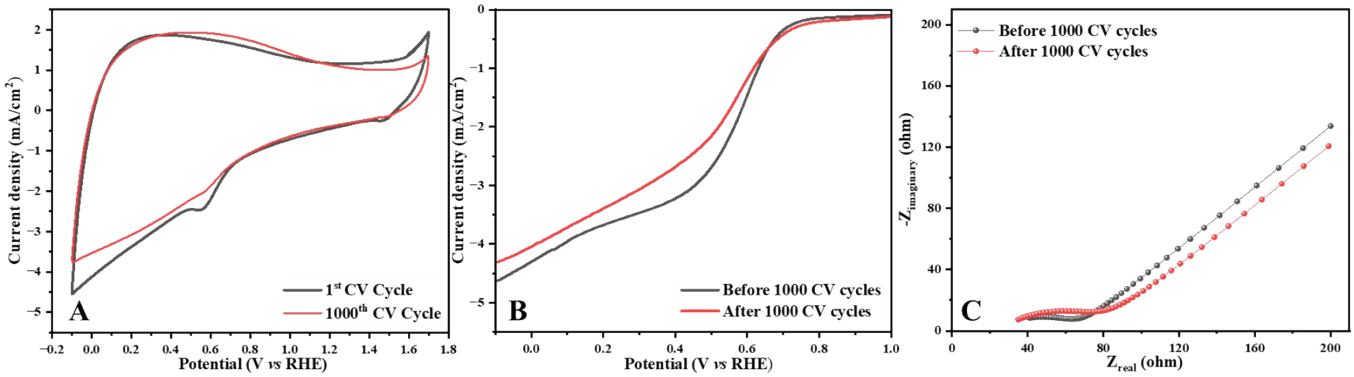

Figure S15. ORR stability analysis of NT@NC-8 catalyst showing (A) 1st and 1000th CV cycle; (B) LSV before and after performing 1000 CV cycles, at 1600 rpm (C) EIS test before and after performing 1000 CV cycles.

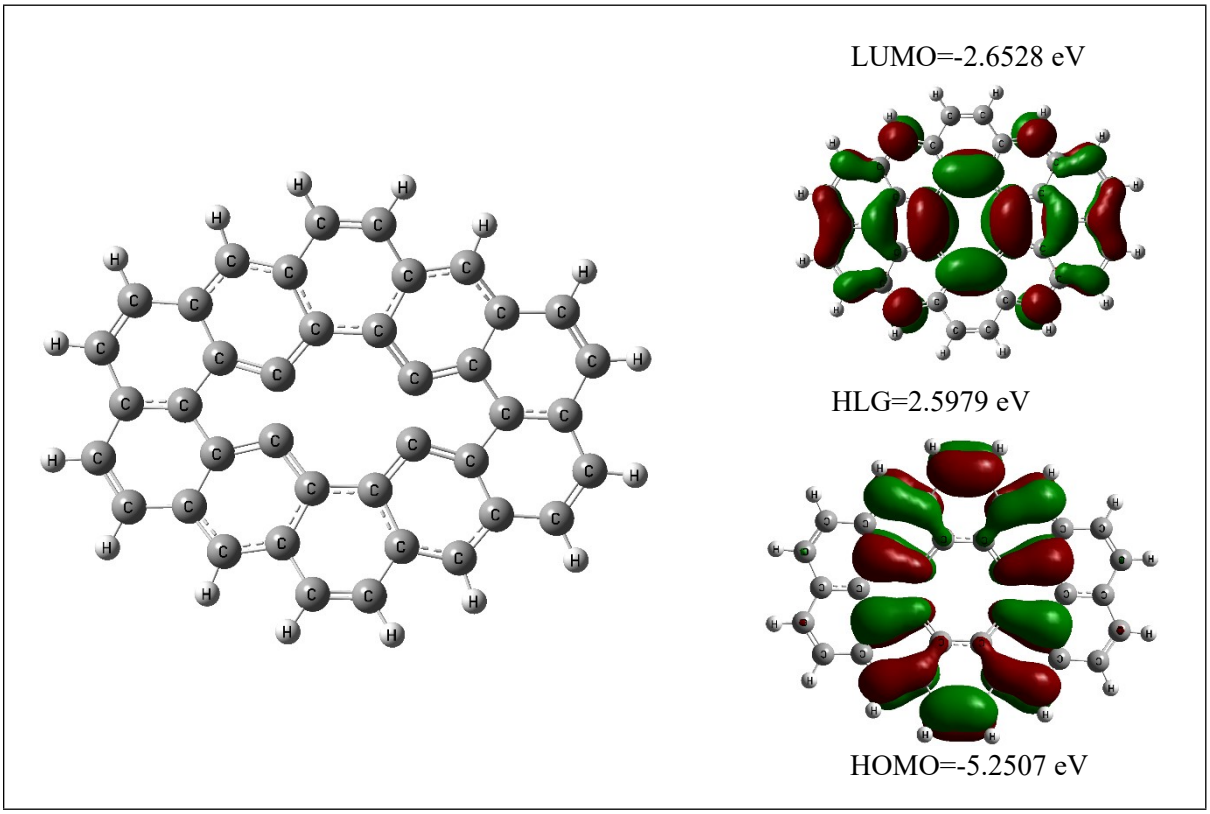

Figure S16. Equilibrated geometry and frontier molecular orbitals of graphitic carbon fragment. (HLG means HOMO-LUMO energy gap)

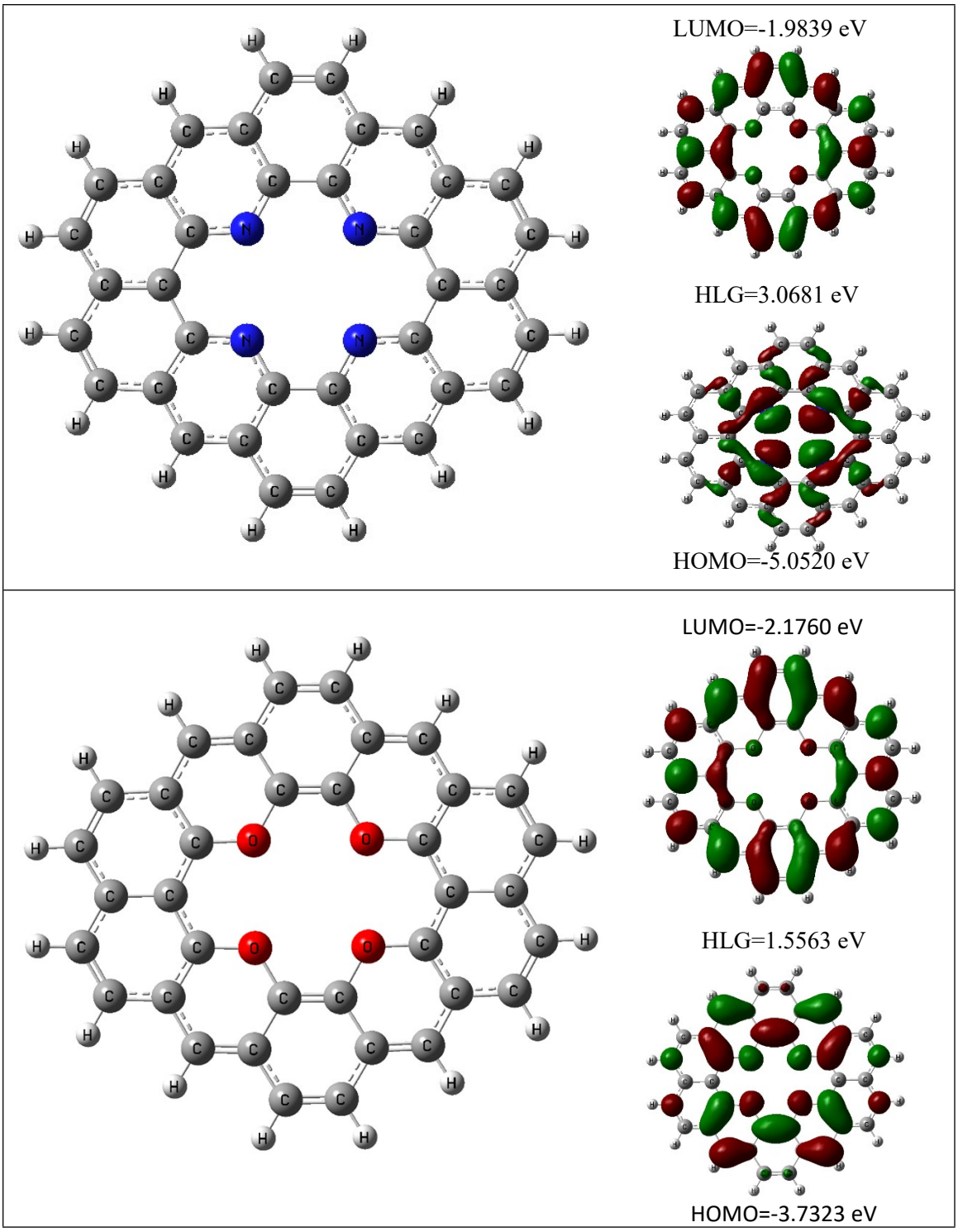

Figure S17. Equilibrated geometry and frontier molecular orbitals of N and O-doped graphitic carbon fragment. (HLG means HOMO-LUMO energy gap)

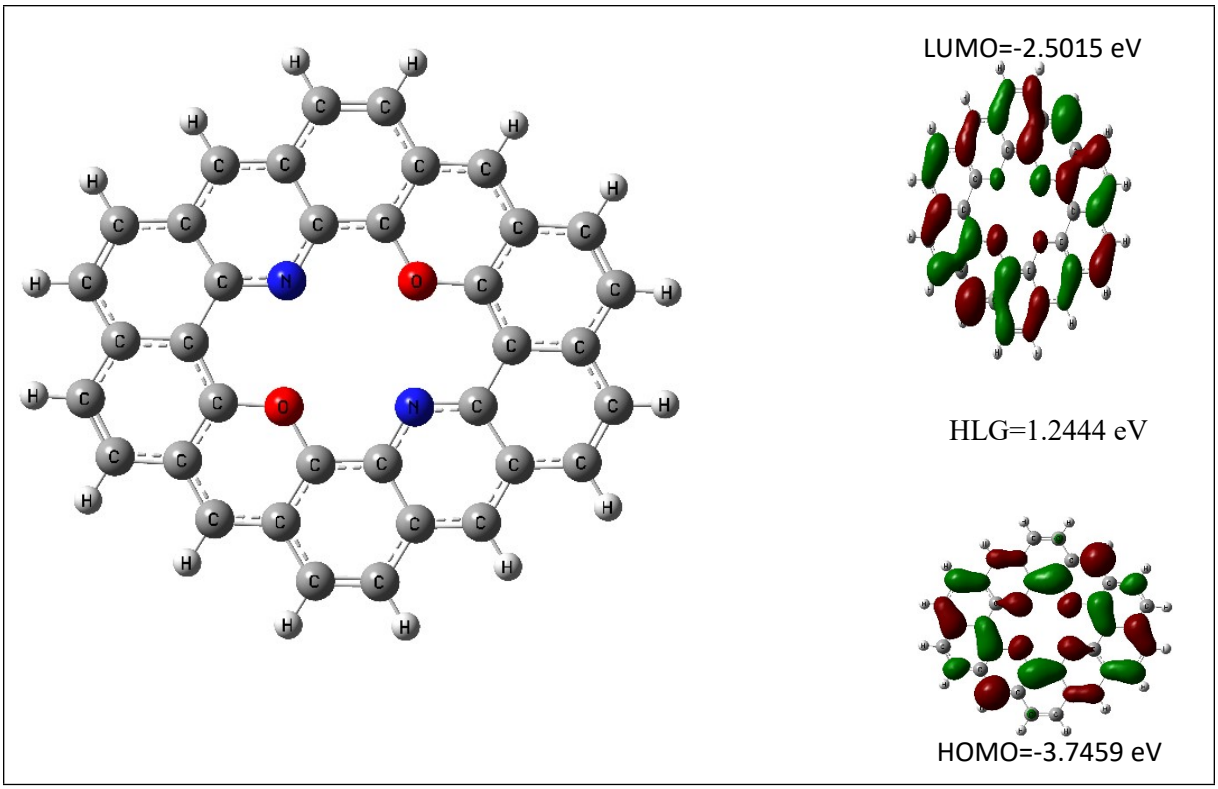

Figure S18. Equilibrated geometry of N and O-doped in an individual carbon fragment and its frontier molecular orbitals. (HLG means HOMO-LUMO energy gap)

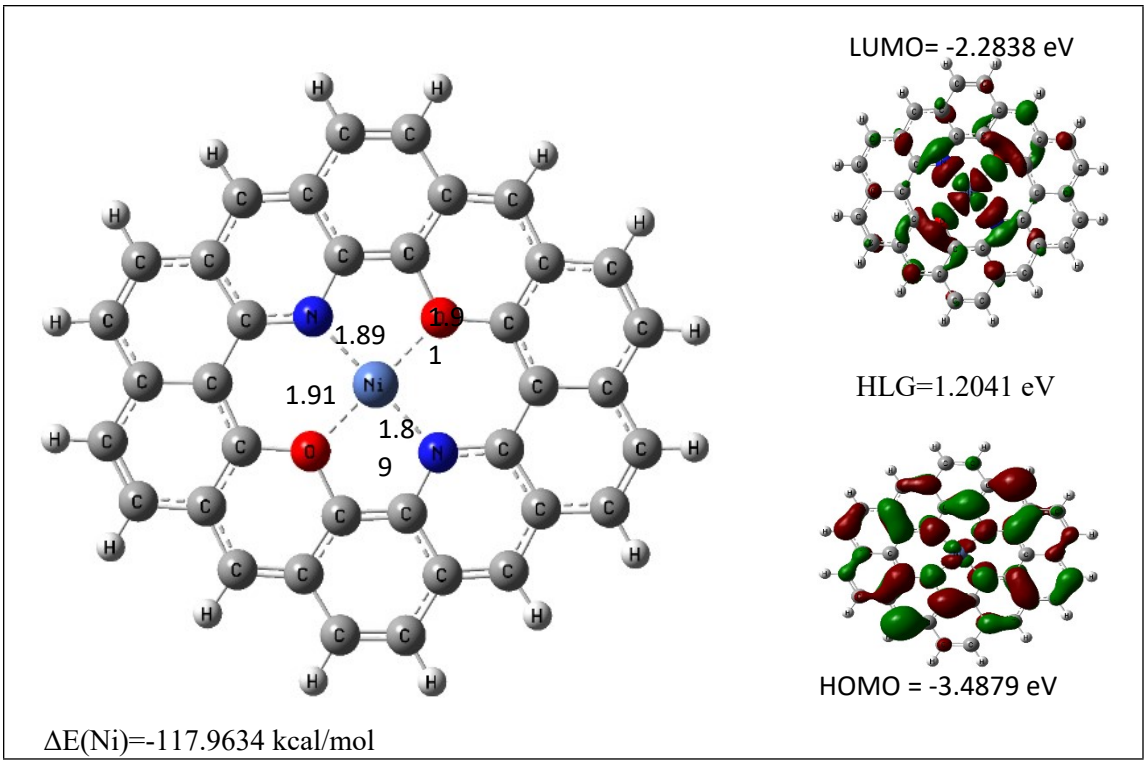

Figure S19. Equilibrated geometry of Ni-encapsulated N and O-doped carbon fragment and its frontier molecular orbitals. (Bond distances are in Å. ΔE means binding affinity. HLG means HOMO-LUMO energy gap)

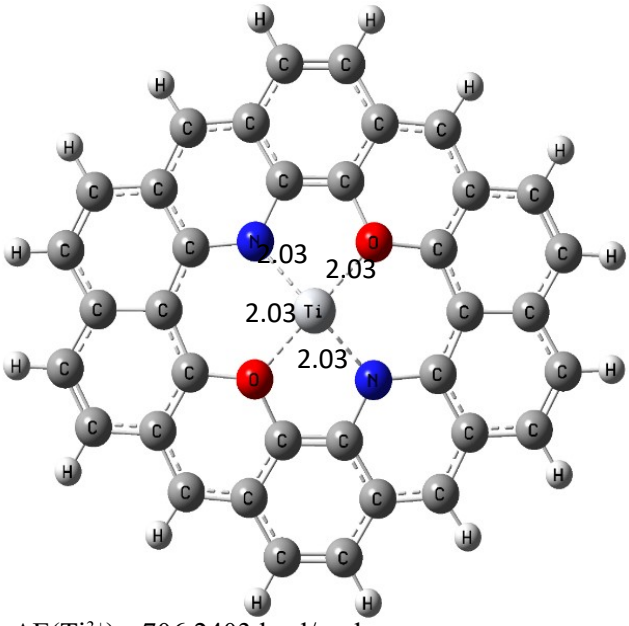

Figure S20. Equilibrated geometry for encapsulation of Ti^{3+} with N and O-doped carbon fragment along with its frontier molecular orbitals. (Bond distances are in Å. ΔE means binding affinity. HLG means HOMO-LUMO energy gap)

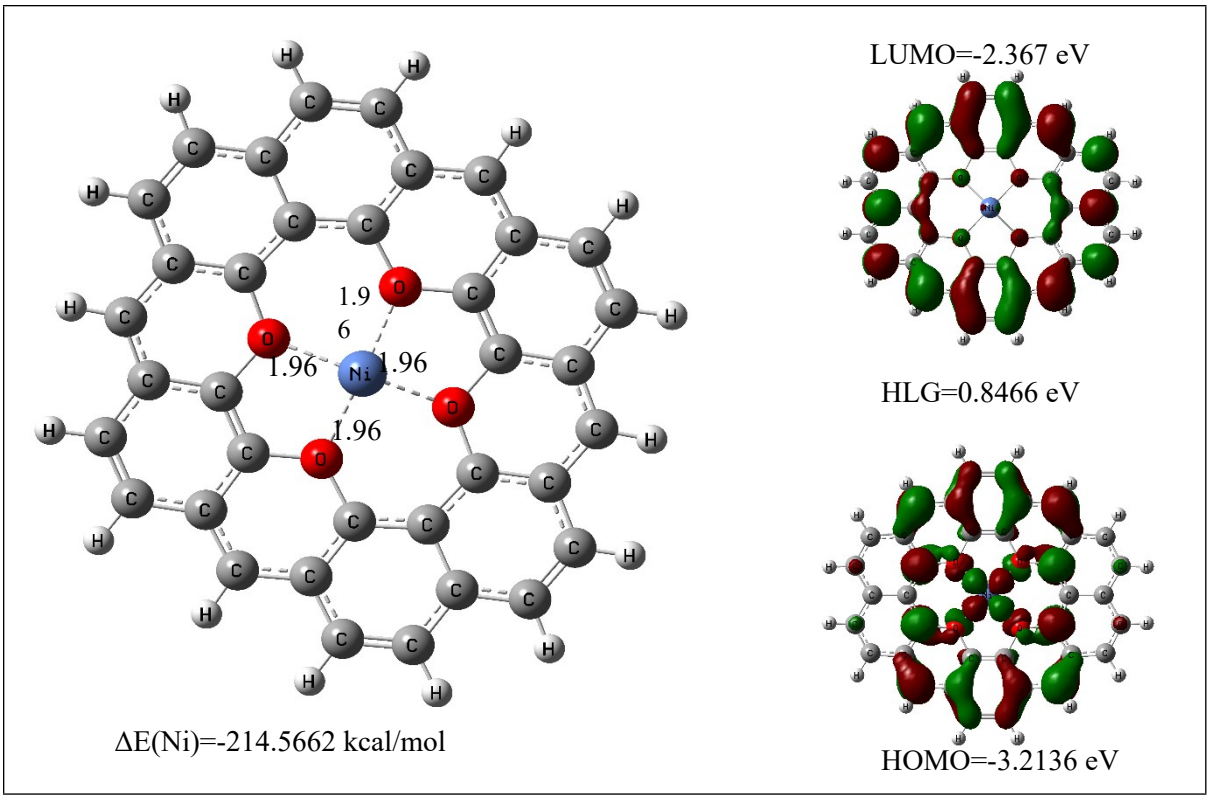

Figure S21. Equilibrated geometry and frontier molecular orbitals for O-doped carbon fragment encapsulating Ni. (Bond distances are in Å. ΔE means binding affinity. HLG means HOMO-LUMO energy gap)

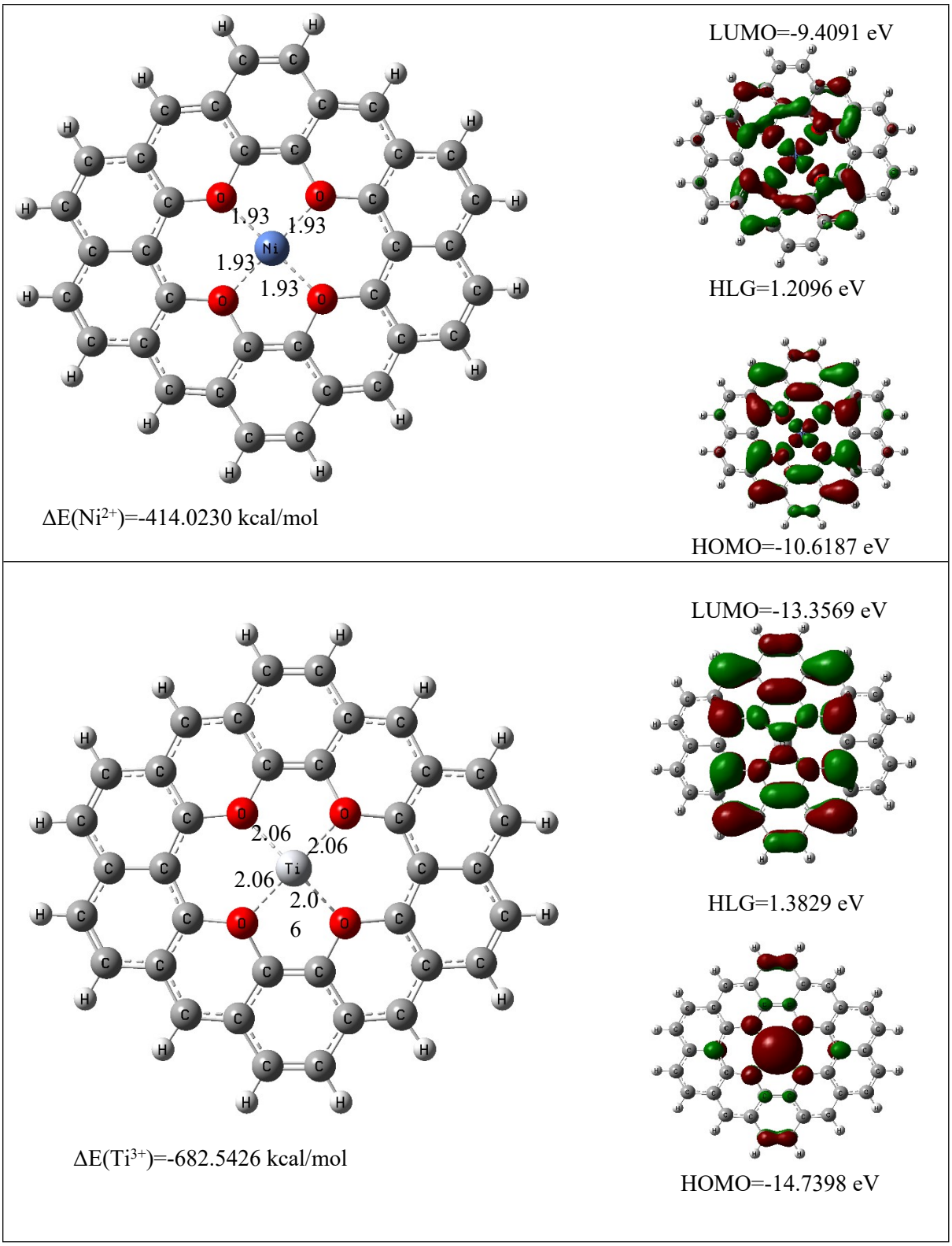

Figure S22. Equilibrated geometry and frontier molecular orbitals for O-doped carbon fragment encapsulating Ni^{2+} and Ti^{3+}. (Bond distances are in Å. ΔE means binding affinity. HLG means HOMO-LUMO energy gap)

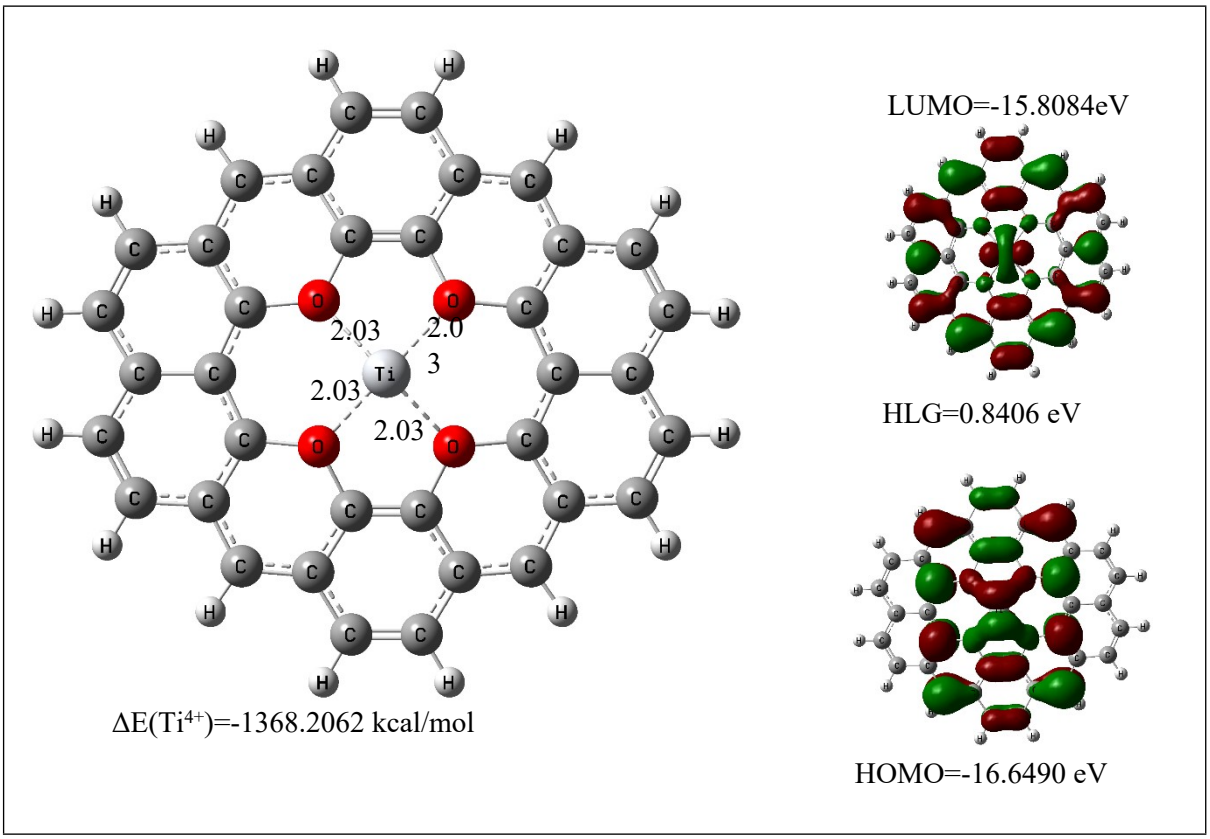

Figure S23. Equilibrated geometry and frontier molecular orbitals for O-doped carbon fragment encapsulating Ti^{4+}. (Bond distances are in Å. ΔE means binding affinity. HLG means HOMO-LUMO energy gap)

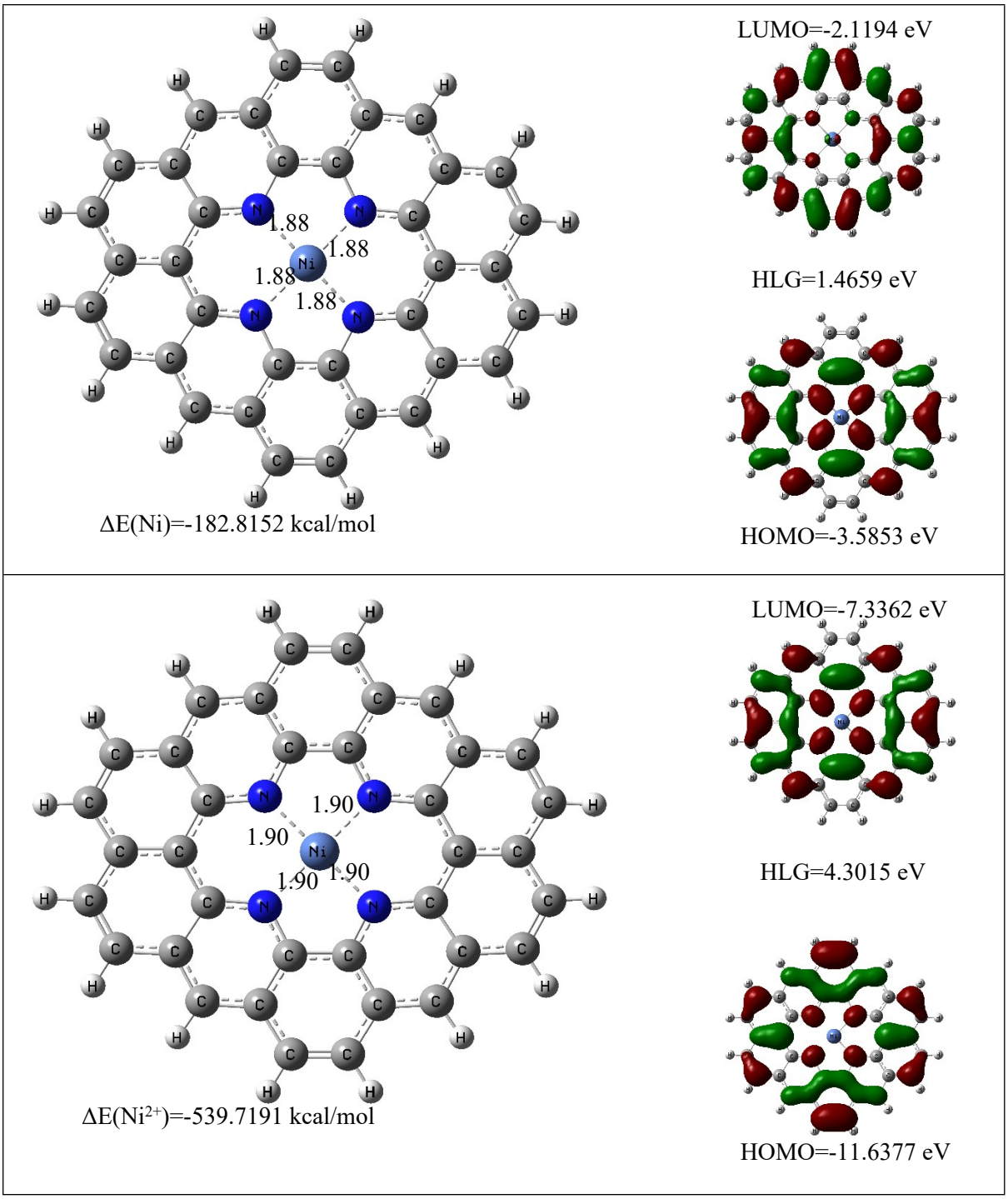

Figure S24. Equilibrated geometry and frontier molecular orbitals for N-doped carbon fragment encapsulating Ni and Ni^{2+}. (Bond distances are in Å. ΔE means binding affinity. HLG means HOMO-LUMO energy gap)

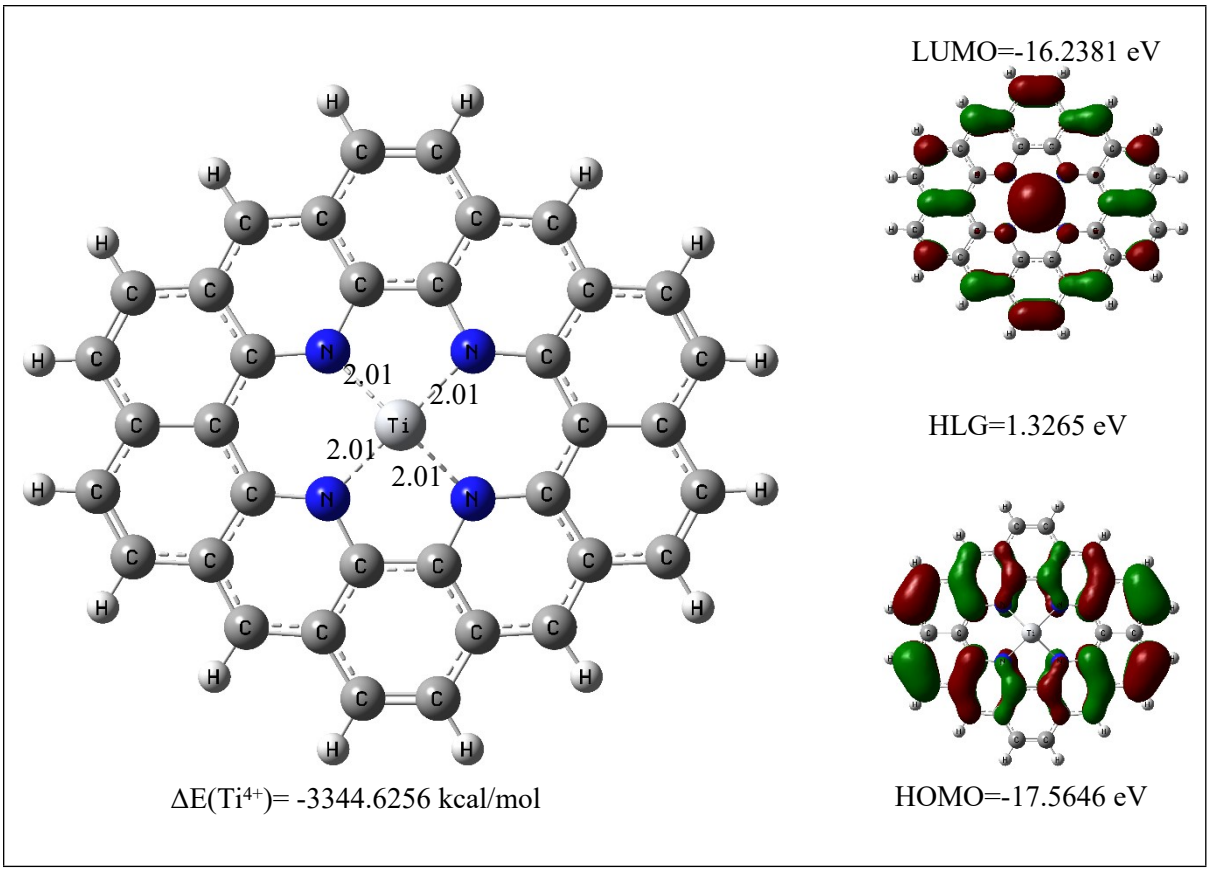

Figure S25. Equilibrated geometry and frontier molecular orbitals for N-doped carbon fragment encapsulating Ti^{4+}. (Bond distances are in Å. ΔE means binding affinity. HLG means HOMO-LUMO energy gap)

Table S1. Table showing the potential and overpotential required by the synthesised materials to achieve OER current density of 10 mA/cm^2 and 50 mA/cm^2 in 1 M KOH with their tafel slopes.

Electrocatalyst	**At 10 mA/cm^2**		**At 50 mA/cm^2**		**Tafel slope (mV/dec)**
	Potential (V vs RHE)	**Overpotential (mV)**	**Potential (V vs RHE)**	**Overpotential (mV)**	
NT@NC-7	1.605	375	1.795	565	82
NT@NC-8	1.585	355	1.695	465	63
RuO_2	1.500	270	1.615	385	64
$Ni(NO_3)_2$	1.693	463	-	-	191
TiO_2	2.301	1071	-	-	207

Table S2. Table showing the charge transfer resistance (R_{ct}) values for the prepared materials in 1 M KOH obtained using EIS.

Catalyst material	**R_{ct} (ohm)**
NT@NC-7	126.58
NT@NC-8	53.20

Table S3. Equivalent fitting parameters of the Randles' circuit for EIS in 1 M KOH.

Catalyst material	**R_s (ohm)**	**R_{ct} (ohm)**	**Q**	**α**	**W (ohm)**	**χ^2**
NT@NC-7	13.153	126.58	5.93E-06	0.852	4538.040	0.042
NT@NC-8	11.599	53.20	3.10E-05	0.648	2506.360	0.109

Table S4. Table with ECSA values of the prepared materials.

Catalyst material	C_{dl} (μF)	ECSA (cm^2)
NT@NC-7	58	1.45
NT@NC-8	178	4.45

Table S5. ICP-MS analysis of the 1 M KOH electrolyte before and after 600 CV cycles performed using NT@NC-8 catalyst to detect nickel metal.

Analyte	Concentration of Nickel (ppm)
1 M KOH before 600 CV cycles	0.000
1 M KOH after 600 CV Cycles	0.000

Table S6. Table with overpotential values for overall water splitting using NT@NC-8 catalyst in 1 M KOH and natural seawater.

Electrolyte	OER overpotential in mV (@10 mA/cm^2)	HER overpotential in mV (@-10 mA/cm^2)
1 M KOH	360	507
Natural seawater	761	733

Table S7: Kinetic parameters of NT@NC-7, NT@NC-8, along with Pt/C, for ORR performed in 0.1 M KOH electrolyte.

Catalyst material	Onset Potential E_{onset} (V vs RHE)	Half-wave Potential $E_{1/2}$ (V vs RHE)	Limiting current density (mA/cm^2)	No. of electrons transferred
NT@NC-7	0.71	0.54	-4.50	3.2
NT@NC-8	0.78	0.64	-5.10	3.9
Pt/C	0.91	0.81	-5.45	3.9

Table S8. Charge transfer resistance of the prepared materials in 0.1 M KOH.

Catalyst material	R_{ct} (ohm)
NT@NC-7	56.66
NT@NC-8	48.57

Table S9. Variation in ORR parameters before and after the stability study using 1000 CV cycles.

ORR in 0.1 M KOH	Before stability cycling	After stability cycling (1000 CV cycles)
Limiting current density (mA/cm^2)	-4.62	-4.32
R_s (ohm)	24.57	25.11
R_{ct} (ohm)	44.08	58.43
Area under CV curve (a.u.)	5.13	4.88

Table S10. Table comparing OER, HER and ORR parameters of the other similar catalysts with that of the prepared catalyst.

S.No.	Electrocatalyst	Electrolyte used in case of OER, HER,and ORR	OER		HER		ORR			Reference
			Overpotential (@10 mA/cm^2) (mV)	Tafel slope (mV/dec)	Overpotential (@-10 mA/cm^2) (mV)	Tafel slope (mV/dec)	Limiting current density (mA/cm^2)	Half wave potential (V)	No. of electrons transfered (n)	
1.	Fe_2P/Fe_3C@NPC	1 M KOH, 1 M KOH, and 0.1 M KOH	440	108.6	97	89.3	4.8	0.87	-	1
2.	2% Ru-NCO	1 M KOH, 1 M KOH, and 0.1 M KOH	269 (@100 mA/cm^2)	59	51	58	-	0.88 V	3.9	2

3.	N-PC@Ni	1 M KOH, 1 M KOH, and 0.1 M KOH	314	312	179	98	-	0.76	3.6	3
4.	PC-$Ni_{0.75}$	0.1 M KOH, 0.1 M KOH, and 0.1 M KOH	368	67.6	297	134.9	4.19	0.67	3.2	4
5.	Co@N-CNTF-2	1 M KOH, 1 M KOH, and 0.1 M KOH	350	61.4	260	-	5.2	0.81	3.96	5
6.	NiFe-NPC	1 M KOH, 0.5 M H_2SO_4, and 0.1 M KOH	306	90	150	103	5.5	0.87	3.95	6
7.	NiCoOS	0.1 M KOH, 0.1 M KOH, and 0.1 M KOH	470	-	300	-	-	0.79	3.9	7
8.	Ni_2P/CoN-PCP	1 M KOH, 1 M KOH, and 0.1 M KOH	270	65	94	41	17.4	0.87	3.9	8
9.	Ni-NC-700	0.1 M KOH, 0.1 M KOH, and 0.1 M KOH	430	100	300	66	-	0.75	4	9
10.	**NT@NC-8**	**1 M KOH, 1 M KOH, and 0.1 M KOH**	**355**	**63**	**326**	**142**	**5.1**	**0.64**	**3.9**	**This work**

References:

1 Y. Li, G. Tang, Y. Wang, Y. Chai, C. Liu, *ACS Omega*, 2022, **7**, 13687-13696.

2 J. Zhang, J. Lian, Q. Jiang, G. Wang, *Chem. Eng.*, 2022, **439**, 135634.

3 C. Sathiskumar, R. Shanmugam, V. Mohanraj, A. Kim, S. Karthikeyan, D.J. Yoo, *Nanomater.*, 2019, **10**, 76.

4 V.C. Hoang, V.G. Gomes, K.N. Dinh, *Electrochim. Acta*, 2019, **314**, 49-60.

5 H. Guo, Q. Feng, J. Zhu, J. Xu, Q. Li, S. Liu, K. Xu, C. Zhang, T. Liu, *J. Mater. Chem. A*, 2019, **7**, 3664-3672.

6 P. Zhang, T. Zhan, H. Rong, Y. Feng, Y. Wen, J. Zhao, L. Wang, X. Liu, W. Hou, *J. Colloid Interface Sci.*, 2020, **579**, 1-11.

7 Z. Bai, S. Li, J. Fu, Q. Zhang, F. Chang, L. Yang, J. Lu, Z. Chen, *Nano Energy*, 2019, **58**, 680-686.

8 T. Sun, S. Zhang, L. Xu, D. Wang, Y. Li, *ChemComm*, 2018, **54**, 12101-12104.

9 B. Devi, R.R. Koner, A. Halder, *ACS Sustain. Chem. Eng.*, 2019, **7**, 2187-2199.